

Optical design of ex-vessel components for the Wide Angle Viewing System diagnostic for ITER

Carmen Pastor^{a,*}, Carmen Rodríguez^a, Mercedes Medrano^a, Alfonso Soletto^a, Ricardo Carrasco^a, Fernando Lapayese^a, A. de la Peña^a, Esther Rincón^a, Santiago Cabrera^a, Augusto Pereira^a, E. de la Cal^a, Fernando Mota^a, Francisco Ramos^a, Vicente Queral^a, Raquel Lopez-Heredero^b, Ana Manzanares^c, Laurent Letellier^d, Sebastien Vives^d, V. Martin^e, Frederic Le Guern^f, J. José Piqueras^f, Martin Kocan^g

^a Laboratorio Nacional de Fusión, CIEMAT, 28040 Madrid, Spain

^b Instituto Nacional de Técnica Aeroespacial, INTA, Torrejón de Ardoz, Madrid, Spain

^c Green Light Solutions, calle de San Bernardo, 20, 28015 Madrid

^d CEA, IRFM, F-13108 Saint-Paul-Lez-Durance, France

^e Bertin Technologies, 155 rue Louis-Armand, CS 30495, 13593 Aix-en-Provence, France

^f F4E, Josep Pla 2, Torres Diagonal Litoral B3, 08019 Barcelona, Spain

^g ITER Organization, Route de Vinon sur Verdon, CS 90 046, 13067 Saint-Paul-lez-Durance, France

ABSTRACT

The equatorial visible and infrared Wide Angle Viewing System (WAVS) for ITER is one of the key diagnostics for machine protection, plasma control and physics analysis. To achieve these objectives, the WAVS will monitor the surface temperature of the Plasma Facing Components by infrared (IR) thermography (3–5 μm range) and will image the edge plasma emission in the visible range. It will be composed of 15 lines of sight installed in four equatorial ports (no. 3, 9, 12 and 17) and will survey more than 80% of the overall area of the vacuum vessel. This paper presents the optical design of the ex-vessel optics, which is at Preliminary Design Status by the time this paper is published. The main function of the ex-vessel optics is to relay the scene image, and also the pupil image, coming from the Port-Plug Optics into a dedicated set of detectors, while keeping the required performance. The optics will work in two bands simultaneously, visible and Mid IR, and will use common refractive optics all along the optical path until it splits into the dedicated sensors at the Port Cell Cabinet. The optical system consists of several modules that comply with the different system interfaces and environmental constraints. A full description of the different modules, its function and performance, and the end to end optics performance will be described in this paper. The optics alignment strategy will be also described and the corresponding assembly and manufacturing tolerances.

1. Introduction

This paper describes the Ex-vessel optical design of the ITER diagnostic 55.G1.C0 Equatorial Visible & Infrared Wide Angle Viewing System (WAVS) in the Equatorial Port #12 and its associated performance.

The WAVS is one of the key diagnostic in ITER devoted to machine protection, plasma control and physics analysis. 15 lines of sight (LoS) composing this diagnostic installed in four equatorial ports (#03, #09, #12 and #17) are foreseen allowing for the monitoring of the surface temperature of the main in-vessel components and imaging the edge plasma emission in the visible range. Port #12 consists of 3 Views, named as Tangential Right View, Tangential Left View and Divertor View. The optics of these three Views will be described in this paper.

For an overview in the progress of the design at previous phases, see references [1–6]

2. Optical design requirements

Table 1 summarizes the main infrared and visible optical specifications used for the assessment of the system measurement performances.

3. Optical design description

Figs. 1 and 2 show the Optics Blocks Diagram and End to End Optical layout, respectively, of one Line-of-Sight of the WAVS (tangential left view). The optical elements of the common path transfer the VIS and IR signals from the Port-Plug through the Interspace and the Bioshield areas up to the Port-Cell. Then, at the very end of the system, and inside the Shielded Cabinet, a beam-splitter splits the two wavebands in order to feed two dedicated channels, each of them having two identical cameras (two identical cameras for the Visible channel and two identical cameras for the IR channel).

3.1. In vessel optics

Complete details of the in-vessel Optics can be found in [6], only a brief description of its components is included here.

In the Port-Plug (Fig. 3), each View is sub-divided in two units:

- The First Mirrors Unit (FMU), with an off-axis ellipsoidal first mirror (M1) which forms an aberrated image close to a second folding mirror (M2)
- The Hot Dog-Leg mirrors Unit (HDL), with a pair of flat folding mirrors (M3 and M4) sending the light through the Windows Assembly (WA), at the exit of the Port-Plug.

See Fig. 3 for a Layout of the Port Plug WAVS Optics.

3.2. Ex vessel optics

Interspace Optics:

See Fig. 4 for a Layout of the Interspace Optics (Divertor View only). As part of the ex-vessel optics the first optical elements are two mirrors facing the PP exit, which constitute the Optical Hinge Unit (OH). This component compensates for the radial and vertical displacements of the Vacuum Vessel (VV) in normal operation and baking. This function will be performed by means of a piezoelectric actuator coupled to the upper mirror of the OH to produce the vertical displacements aimed at the alignment of the optical beam. Following the OH, the ORU (Optical Relay Unit) relays the beam reducing its diameter and producing a collimated beam that enters the interspace optics. The optical elements of the Port Plug, OH and ORU are all reflective. Regarding mirror materials and coatings, these are still under consideration being Zerodur or fused silica the current candidates for the mirror substrate. A dedicated test campaign for several substrates materials and mirror coatings has been conducted at previous phases [7].

Right after the ORU, we find the Interspace Afocal Module 1. It is a refractive optical system that consists of two identical doublets that relays the pupil ahead, controlling at the same time the beam diameter. The first doublet produces a real image at half way of the optical system. The second doublet acts as a collimator that produces a collimated exit beam that propagates towards the Bioshield (BS). The afocal module 1, is a Keplerian telescope with magnification 1X (in all views).

BioshieldOptics:

Inside the Bioshield, two flat mirrors tilted at 45° constitute a radiation shielding Cold Dog Leg (CDL) and will allocate alignment capability for the LoS. Following the CDL, a doublet focuses the collimated beam and produces a real scene image inside the Bioshield, such that the beam diameter is kept under control along the optical system. This

refractive module is also a Keplerian telescope afocal module, with magnification 1X for both Tangential Views, a 1.39X for the Divertor View. See Fig. 5 for a Layout of the Bioshield Optics (Divertor View only).

Port Cell Optics:

See Fig. 6 for an optics layout of the Port Cell area (Divertor View only).

In the Port Cell area (PC), the optical design concept is also refractive, except for the folding mirrors and the beam splitting components. Part of the optics is installed outside of the shielded cabinet. This module is named as Afocal Module 3, and it is also a Keplerian telescope with magnification 1.92X for the Tangential Right View, 2.3X for the Tangential Left View, and 0.97X for the Divertor View. It includes 2 folding mirrors in the path that help to accommodate the entry of the beam into the shielded cabinet. The first optical element inside the cabinet, common to the IR and the VIS channels, is a dichroic beamsplitter at 45° that separates the radiation between the IR and the VIS spectral range by transmitting in the IR and reflecting in the VIS. The camera optical elements are inside the shielded cabinet where the cameras are located. The Visible Objective is a set of 4 lenses focusing the beam at the sensor focal plane. The design allows for the implementation of a second camera, producing an extra image in real time. This is achieved by beam splitting a second time in the optical train. A third beam splitter (or dichroic) is implemented in the design which allows two operational IR cameras that provide redundancy for temperature measurements. The IR objective is also refractive and consists of 5 lenses. The optical interface with the detector foresees the implementation of a cooled sensor and includes a pupil image at the vicinity of the focal plane (cold stop). The focal length of each camera objective is shown in Table 2.

Table 1
Infrared & Visible optical specifications.

WAVS Optics main requirements	Divertor View		Tangential Left View		Tangential Right View	
	IR	VIS	IR	VIS	IR	VIS
HFOV x VFOV (°)	36.1° x 45°		43° x 53.8°		21.5° x 26.9°	
Detector size	1024 x 1280 pixels of 15 µm	1728 x 2236 pixels of 7 µm	512 x 640 pixels of 15 µm	1024 x 1280 pixels of 7 µm	512 x 640 pixels of 15 µm	1024 x 1280 pixels of 7 µm
Equivalent Focal Length	23.57 mm	19.74 mm	9.75 mm	9.1 mm	20.23 mm	18.88 mm
Entrance Pupil Diameter	4,6 mm		4 mm		4 mm	
F-number	5.12	4.3	2.44	2.3	5.06	4.7
Spectral Range	4 ± 0.1 µm	656 nm ± 1 nm	4 ± 0.1 µm	656 nm ± 1 nm	4 ± 0.1 µm	656 nm ± 1 nm
Optical Transmission	>8%	>2%	>8%	>2%	>8%	>2%
Enclosed Energy (IR) MTF (VIS)	EE> 50% within 2x2 pixels of 15µm	MTF>20% at 70cy/mm (Nyquist)	EE >50% within 2x2 pixels of 15µm	MTF>20% at 70cy/mm (Nyquist)	EE>50% within 2x2 pixels of 15µm	MTF>20% at 70cy/mm (Nyquist)

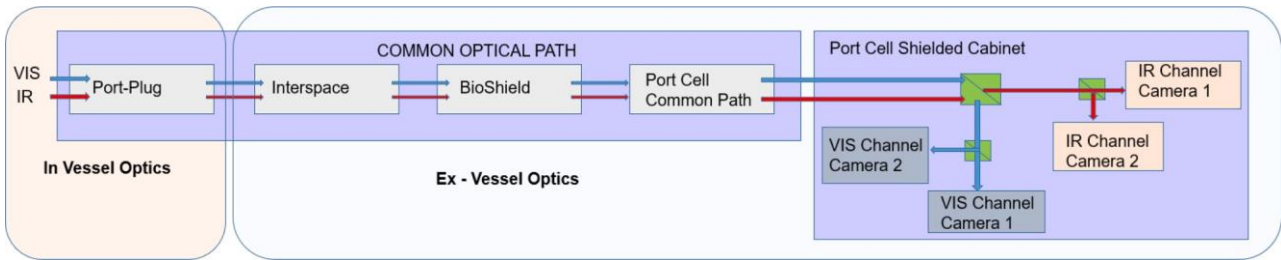


Fig. 1. WAVS optics blocks diagram.

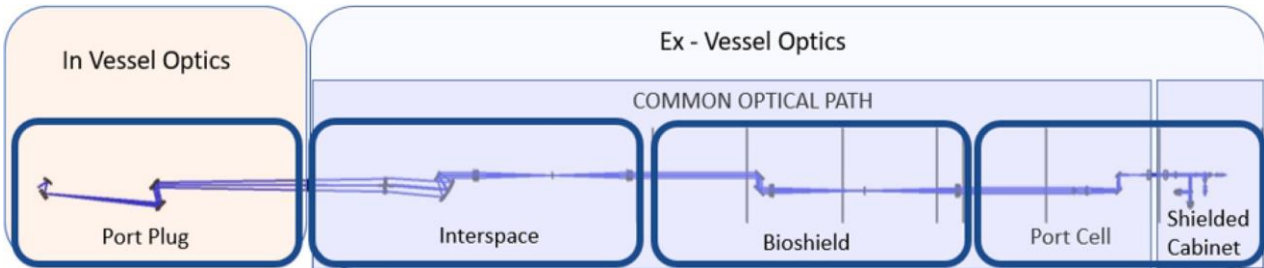


Fig. 2. . End to end tangential left view optical layout.

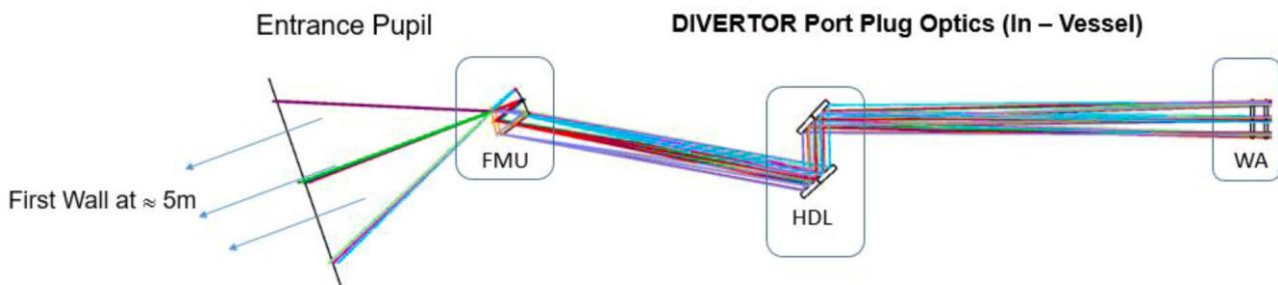


Fig. 3. Port plug WAVS optics. Divertor view.

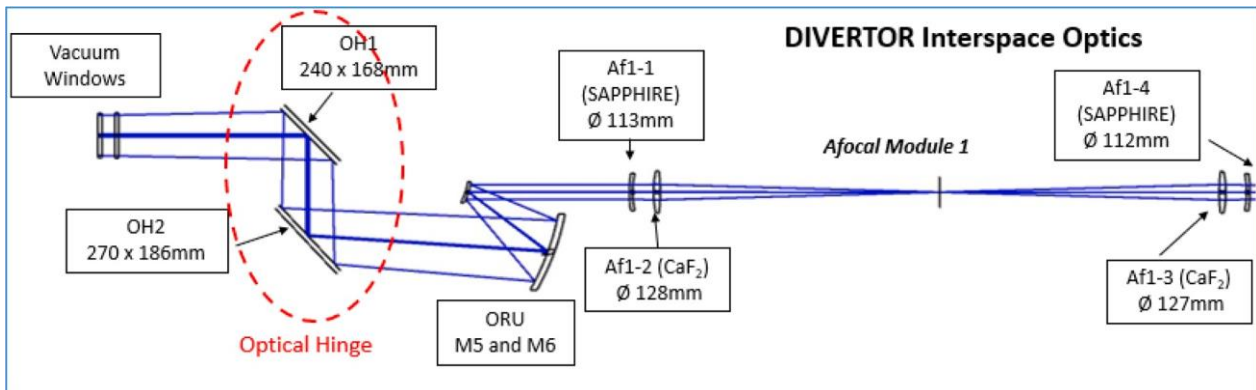


Fig. 4. Interspace optics. Divertor view.

3.3. Use of refractive optics

Restrictions in the available space for the Ex-vessel optics, led us to discard the use of reflective optics for the optical design of WAVS. With this, the main advantage of the use of reflective optics is also missed, and

that is the multispectral capability of a mirror-based optical system. A refractive optical system has been implemented instead. Besides, to reduce the number of elements, most of the optics works in dual band in a common optical path that goes from the Interspace Area to the Shielded Cabinet in the port Cell Area.

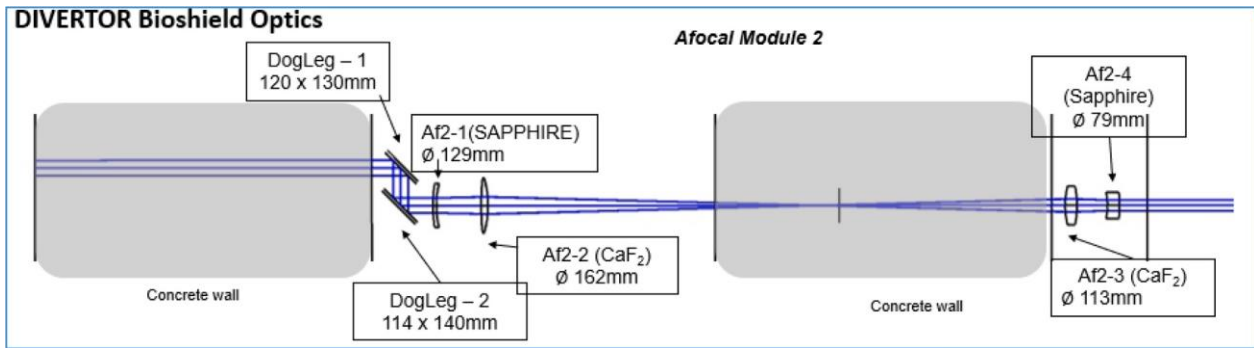


Fig. 5. Bioshield optics. Divertor view.

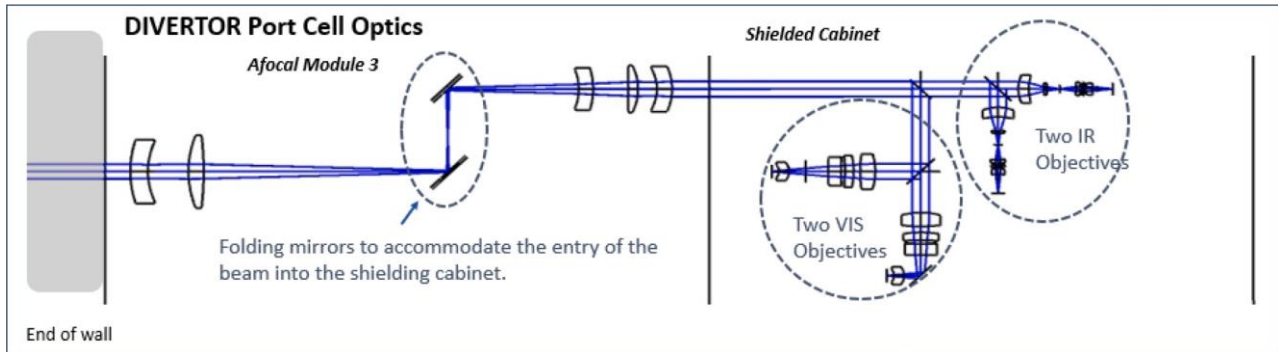


Fig. 6. Port cell optics. Divertor view.

Table 2
Objective optics focal length.

Objective Optics Focal Length	MWIR	VISIBLE
TAN RIGHT	100.3 mm	100.7 mm
TAN LEFT	49.4 mm	52.3 mm
DIVERTOR	152.7 mm	139.2 mm

Working in dual band with common refractive optics for both bands is an obvious advantage from the reduction in optical elements point of view. Nevertheless, due to the difference in the index of refraction of the optical materials for the different wavelengths, a different response and correction of the aberrations is inherently present. The main consequence that arises from this is the chromatic aberration. To reduce this effect a narrowing of the spectral bands has been implemented and accepted as valid, and therefore the optics will be reaching the specified operational performance when working at $4 \mu\text{m} \pm 0.1 \mu\text{m}$ for the MWIR and $656 \text{ nm} \pm 1 \text{ nm}$ for the visible.

Also, the materials used in the optical elements have been chosen taking into account their good performance under the harsh environmental conditions identified in the equatorial ports location in terms of radiation, temperature and humidity. A dedicated test campaign for several materials and coatings has been conducted at previous phases [8, 9].

3.4. Optics modularity. Optical interfaces

A big improvement in time and cost in several subsequent activities can be achieved when using optically corrected and independent optical modules along the optical path. In this way the independent modules or subsystems can be assembled, integrated and verified as independent optical systems, such that they don't need to be installed on site for its verification, check or maintenance tasks. This is the strategy followed for the optical design of ex-Vessel Optics of WAVS. The optical system of

each view consists of 3 afocal modules plus the cameras objectives, and each of them is independently corrected.

3.5. OH optomechanical tolerancing study and implementation of focus capability

During operation of the reactor, the Vacuum Vessel is affected by radial and vertical thermal dilatations which produce relative displacements between the optical components inside the Port Plug and the ex-vessel optics.

These relative displacements have an impact on the optical performance, degrading the image quality and decentering the Line of Sight (LoS). These effects must be corrected by means of a set of two mirrors attached in an Optical Hinge (OH).

Making use of the very similar deformation produced by the thermal effects in both axis (radial and vertical), the linear vertical movement of the upper mirror of the Optical Hinge (mirror OH1) will produce the

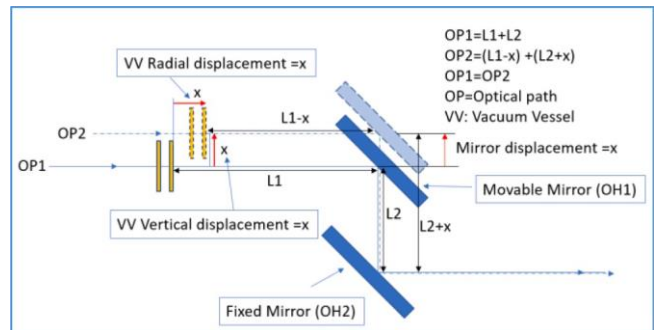


Fig. 7. Optical Hinge optical correction function layout.

desired correction in both focus and alignment with a single movement. See Fig. 7 for a layout of the optical correction implemented by the mirror displacement.

The positioning of the movable mirror (upper movable mirror (OH1) in Fig. 7) can adopt three fixed positions, corresponding to three established temperature modes; operational, baking and ambient temperature. This means that no real-time corrections are foreseen with this mirror. Then, any deviation of the Vacuum Vessel deformations from the nominal values can mean a degradation of the optical performance of the WAVS, as the OH1 mirror will only have one of the pre-set fixed positions. This section describes the results of the assessment done on the range of tolerance in the positioning of OH1, while keeping the optical performance under control. The need of a refocusing device is also considered here, such that a complementary correction can be added to the system and in that way residual defocus correction can be implemented in real time. The study concludes that the tolerance in position of the OH1 mirror is not critical (several mm of positioning errors does not affect the performance). It also showed a reduced sensitivity or low efficiency of the OH1 mirror, when used for refocussing purposes. A fine focusing mechanism is then proposed for the complete optical system to correct defocusing, and this will be implemented at the end of the optical system, at the camera objective optics.

An additional conclusion of this study shows that a residual LoS decentering is always present when correcting with the OH1 mirror. For Alignment/ Decentering correction, the OH mechanism could be used, in open loop, depending on the allowed tolerance on image decentering.

4. Optomechanical tolerancing

The Tolerancing Study included in this document correspond to the Ex-Vessel Optics only, such that the Port Plug and ORU optical systems are contributing as with its nominal performance only, and no degraded contribution from this optical module to the final tolerancing results is taken into account here. End to End Performance for the as-built system (including the PP and ORU optical modules) will be reported at the Final Design Review phase.

The main Software tool used for the tolerancing study has been Zemax OpticStudio.

The tolerances available for analysis include variations in construction parameters such as curvature, thickness, position, index of refraction, Abbe number, aspheric constants, irregularity of surface shape, etc. The study also supports analysis of decentration of surfaces and lens groups. The various tolerances may be used in any combination to estimate alignment and fabrication error effects on system performance. This has been chosen such that follows the assembly and alignment strategy we have in mind for the WAVS End to End System. The tolerancing analysis is critical to define a representative fabrication and assembly budget in terms of integration times and cost.

Regarding the feasibility of the study, exact ray tracing is used for tolerance analysis. There are no approximations or extrapolations of first order results in the tolerance algorithms used.

Tolerances may be evaluated by several different performance criterion, we have used two different Tolerancing runs: RMS wavefront error and boresight or LoS error (through a user defined merit function). Additionally, compensators have been defined to model allowable adjustments made to the lens after fabrication. Limits in the range of compensation have been placed for the chosen compensators.

The way the tolerances have been computed and analyzed is by a Sensitivity Analysis: for a given set of tolerances, the change in the chosen criterion is determined for each tolerance individually. Also, the criterion for each field and configuration (or channel) individually has been computed. The sensitivity analysis considers the effects on system performance for each tolerance individually. The aggregate or total performance is then estimated by a root-sum square calculation, such that this represents a worst case scenario.

We have also considered an alternative approach to the computation of tolerances, by a Monte Carlo Analysis: this is an alternative way of estimating aggregate effects of all tolerances. This simulation generates a series of random lenses which meets the specified tolerances, then evaluates the criterion. No approximations are made other than the range and magnitude of defects considered. By considering all applicable tolerances simultaneously, an exactly, highly accurate simulation of expected performance is possible. The Monte Carlo simulation can generate any number of designs, using normal, uniform, parabolic, or user defined statistics. For the study presented here a normal distribution statistic has been used.

The performance criteria is the following:

Optics MTF (visible) to demonstrate the compliancy with the requirement: >20% at 70 cycles/mm

Ensquared Energy (IR) to demonstrate the compliancy with the requirement: >50% within 2×2 pixels. Boresight (LoS deviations): less than 2% of the FoV.

4.1. Manufacturing and assembly tolerances

A summary the general tolerances and compensators applied to the optical and optomechanical elements is shown in Tables 3 and 4. The chosen set of tolerances guarantees that the specified image performance and LoS accuracy can be achieved. Two types of quality compensators are considered; image quality compensators and boresight (or LoS) compensators (Table 5).

4.2. Operational tolerances

The study of the operational tolerances shows the potential errors produced during the system operation and its effect on both the Image quality and Line of Sight deviations. The assessment consists of the identification of the degradation produced with the change of temperature, within the specified temperature range from 18 to 35 °C. Gravity effects are also considered in the structural deformations. The study has two parts: Thermo-Optical effects and Thermo-Structural effects.

4.2.1. Thermo optical effects

As mentioned in Section 3.3, "Use of refractive optics" the common path materials choice for the Ex-vessel optical design is very limited and its behavior highly limits the optimization degrees of freedom.

The optical parameters susceptible of change with temperature such as the index of refraction of the lenses substrate also behave different for both spectral bands and a dedicated study has been done on this.

In Fig. 8, the change in the index of refraction with temperature is

Table 3

Expected deformations in the vacuum vessel for 2 different scenarios.

Temperature	Direction of displacement	Displacement
100 °C	u_{rad} (R→)	15.40 mm
	u_{tor}	0
	u_{vert} (Z ↑)	15.06 mm
200 °C	u_{rad} (R→)	36.16 mm
	u_{tor}	0
	u_{vert} (Z ↑)	36.46 mm

Table 4

Tolerances of WAVS ex-vessel optical system.

Tolerances	Lenses & Mirrors	Mechanical Elements
SURF.SHAPE	$\approx 1\lambda$ p-v	NA
THICKNESS	$\pm 50 \mu\text{m}$	± 50 – $200 \mu\text{m}$
SEPARATION	± 50 – $100 \mu\text{m}$	± 50 – $100 \mu\text{m}$
TILT	± 1 – 4 arcmin	NA
DECENTERING	± 50 – $100 \mu\text{m}$	NA

Table 5

Quality compensators of WAVS ex-vessel optical system.

Compensation of LoS or Boresight	While Assembly & Alignment Compensator	Range	Accuracy	While Operating Compensator	Range	Accuracy
	Detector	±0.5 mm (decentering)	<25–50 μm	OH1 mirror	±40 mm (vertical)	<200 μm
	Cold Dog Leg Mirror	±5 mm (decentering)	<200 μm			
	Afocal modules	1–2 mm (decentering)	<100 μm			
Image quality	Doublets in Afocal Modules	±1.5 mm (focus)	<20 μm			
	Focusing Mechanism	±0.8 mm (focus)	<2 μm	Focusing Mechanism	±1 mm (focus)	<2 μm

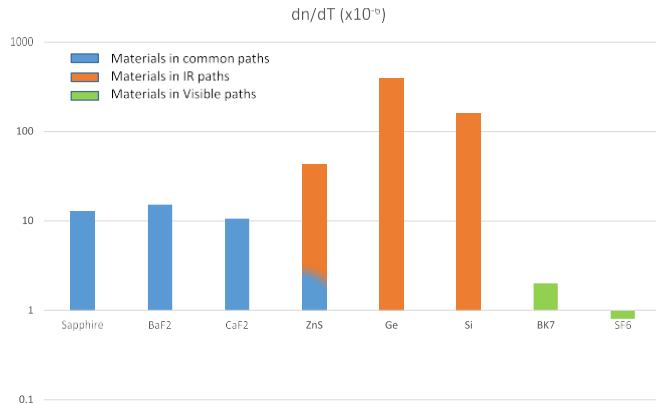


Fig. 8. dn/dT for the optical materials used in WAVS.

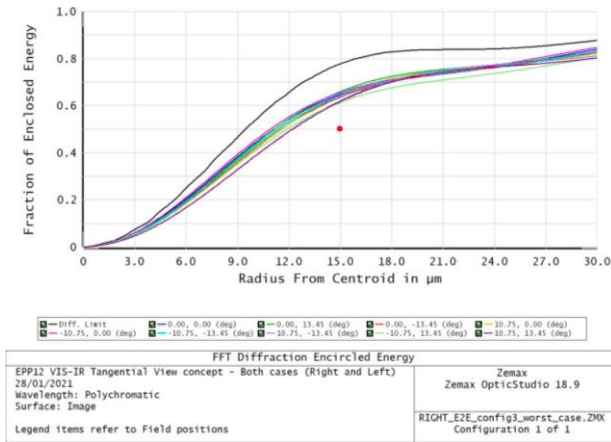


Fig. 9. Diffraction EE for the as-built E2E system. TAN RIGHT view (IR). Red dot indicates Spec. value. (For interpretation of the references to color in this figure legend, the reader is referred to the web version of this article.)

shown in a comparative graph for each material used in WAVS, and in logarithmic scale. It can be appreciated the big difference in the behavior of the change of the index of refraction with Temperature in the materials used for the visible path, with respect to the ones in the IR path. Additionally, and regarding the common optical path, this behavior is spectral-sensitive, so the change is slightly different for each spectral band, and therefore this is an additional impact on the materials available to use in the common path. Data in the graph has been taken from different manufacturers and Zemax materials catalog.

A thermo-optical simulation has been run with Zemax, and its effect on the imagen degradation has been assessed for WAVS. As a good approximation these temperature errors can be considered linear errors, such that its effect on the image performance can be approximated as a defocusing. The optical End to End system provides a refocusing

mechanism (in the cameras optics) which can be used to compensate for the linear errors produced in this temperature scenario. The study shows that the needed range of refocusing to compensate for the thermo-optical errors is within the total operational-working movement of the focusing mechanism, and specifically around ±0.5 mm for all views.

4.2.2. Thermo structural effects

The output of the Thermo - Structural analysis (not included here) is used to estimate the degradation on the Image quality and Line of Sight deviations with the operational temperatures. The considered range in temperatures has been from 18 °C to 35 °C. The analysis is made separately for each optical module. A worst case scenario, which is at both ends of the temperature range, and statistics is taken, such that the degradation values (defocusing and LoS errors) for each module are Root Summed Squared, and the resulting figure is reported. The results are the following:

- Refocusing needed < ±0.1 mm for all views and channels
- LoS errors: Between 5 and 17 pixels, depending on each view and channel

These values are taken into account as contributors in the complete tolerancing study, and they are not considered as a potential problem.

5. Image performance

Fig. 9 and Fig. 10 show the optical MTF and Ensquared Energy (EE) for the as built (after tolerancing) End to End. For this simulation a Monte Carlo approach has been adopted to construct the as-built optical system. The results are shown for the Tangential Right view only. An indication of the specified value is also indicated in both graphs.

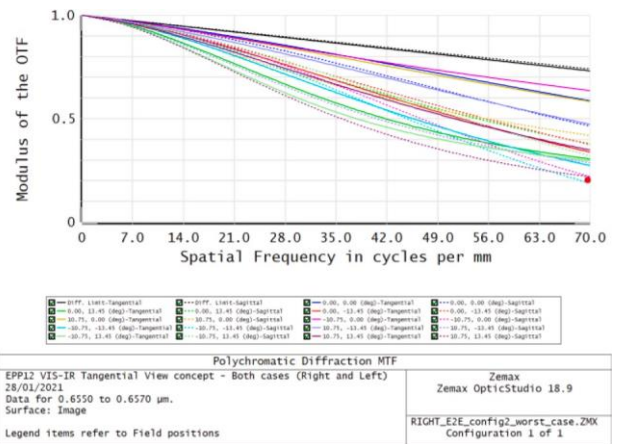


Fig. 10. Optical MTF for the as-built E2E system. TAN RIGHT View (VIS). Red dot indicates Spec. value. (For interpretation of the references to color in this figure legend, the reader is referred to the web version of this article.)

6. Conclusions

WAVS Optics has reached its Preliminary Design Phase and the design overview solution is shown here. The total length of the WAVS Ex-vessel Optical System is around 10 m, from the exit of the vacuum Vessel to the very end of the Shielded Cabinet. The required focal length of the optics in this volume, is only 10–20 mm. With this, a priori, contradictory magnitudes, the optical system must relay both the pupil image and the scene image of the system all along the optical path, while keeping the optical beam at a reasonable size and controlling the aberrations at the same time. One of our main goals in the optical design of WAVS has been the development of a robust, manufacturable and operation-tolerant optical system. Additionally, a big improvement in time and cost in several subsequent activities can be achieved when using optically corrected and independent optical modules along the optical path. In this way the independent modules or subsystems can be assembled, integrated and verified as independent optical modules, such that reduced optical equipment will be needed on site.

Declaration of Competing Interest

The authors declare that they have no known competing financial interests or personal relationships that could have appeared to influence the work reported in this paper.

Acknowledgments

This work was performed with Fusion for Energy and their partial

financial support in the framework of the contract F4E-FPA-407. The views and opinions expressed herein do not necessarily reflect those of Fusion for Energy nor those of the ITER Organization.

References

- [1] S. Salasca, Development of equatorial visible/infrared wide angle viewing system and radial neutron camera for ITER, *Fusion Eng. Des.* 84 (7–11) (Jun. 2009) 1689–1696, <https://doi.org/10.1016/j.fusengdes.2008.12.088>, nos.
- [2] S. Salasca, Recent technical advancements of the ITER equatorial visible/InfraRed diagnostic, *Fusion Eng. Des.* 86 (6–8) (Oct. 2011) 1217–1221, <https://doi.org/10.1016/j.fusengdes.2011.02.015>, nos.
- [3] R. Reichle, Concept development for the ITER equatorial port visible/InfraRed wide angle viewing system, *Rev. Sci. Instrum.* 83 (10) (Oct. 2012) 10E520, <https://doi.org/10.1063/1.4734487>, Art. no.
- [4] S. Salasca, The ITER equatorial visible/infra-red wide angle viewing system: status of design and R&D, *Fusion Eng. Des.* 96–97 (Oct. 2015) 932–937, <https://doi.org/10.1016/j.fusengdes.2015.02.062>.
- [5] L. Letellier, System level design of the ITER equatorial visible/infrared wide angle viewing system, *Fusion Eng. Des.* 123 (Nov. 2017) 650–653, <https://doi.org/10.1016/j.fusengdes.2017.06.005>.
- [6] S. Vives, Overview of optical designs of the port-plug components for the ITER Equatorial Wide Angle Viewing System (WAVS, *Fusion Eng. Des.* 146 (Sep. 2019) 2442–2445, <https://doi.org/10.1016/j.fusengdes.2019.04.014>.
- [7] A Pereira, Steam-resistant optical materials for use in diagnostic mirrors for ITER, *IEEE Trans. Plasma Sci.* 48 (6) (June 2020).
- [8] R.M. Almazán et al., “Test report - steam ingress and humidity test of the WAVS optical samples” ITER IDM ITER_D_UVXNCU v1.0. 2, July 2017.
- [9] J.A. Gonzalo, Environmental, Gamma Radiation and Steam Ingress Tests on Optical samples. Summary of the Results Obtained for the WAVS Diagnostic, et al., 33rd ITPA Diagnostics, ITER, France, 2017.